



# A Novel Fluorescent Probe Based on Pyrazole-Pyrazoline for Fe (III) Ions Recognition

Ying-Peng Zhang<sup>1</sup> · Xiang-Fang Li<sup>1</sup> · Yun-Shang Yang<sup>1</sup> · Jing-Li Wang · Yu-Chen Zhao<sup>1</sup> · Ji-Jun Xue<sup>2</sup>

Received: 5 August 2020 / Accepted: 5 October 2020 / Published online: 13 October 2020  
© Springer Science+Business Media, LLC, part of Springer Nature 2020

## Abstract

Firstly, a novel pyrazole-pyrazoline fluorescent probe was developed and synthesized. The probe can be used to determine Fe<sup>3+</sup> ions in a series of cations in tetrahydrofuran aqueous solution with high selectivity and high sensitivity. After the addition of iron ions, the fluorescence intensity is significantly reduced. Its structure was characterized by <sup>1</sup>H NMR, <sup>13</sup>C NMR and HR-ESI-MS. UV absorption spectra and Fluorescence spectroscopy were used to study the selective recognition of probe **M** on metal ions. The probe **M** can selectivity and sensitivity to distinguish the target ion from other ions through different fluorescence phenomena. In addition, the binding modes of **M** with Fe<sup>3+</sup> were proved to be 1:1 stoichiometry in the complexes by Job's plot, IR results. The combination of probe **M** and iron ions is 1:1, and the detection limit is  $3.9 \times 10^{-10}$  M. The binding mode and sensing mechanism of **M** with Fe<sup>3+</sup> was verified by theoretical calculations using Gaussian 09 based on B3LYP/6-31G(d) basis.

**Keywords** Fluorescent probe · Fe<sup>3+</sup> ion · Recognition · Pyrazoline · Pyrazole

## Introduction

Metal ion fluorescent probes have received extensive attention due to their wide application in environmental and biochemical fields [1]. Fe<sup>3+</sup> ion is one of the essential ions for life. Many cell-level biochemical processes require the participation of iron ions [2, 3]. Therefore, the research on the detection of iron ions is of great significance in the environment and life sciences. The lack or excess of Fe<sup>3+</sup> can induce many diseases, such as diabetes, hepatitis, anemia and Parkinson's disease [4–6], so it is very important to detect Fe<sup>3+</sup>. Commonly used detection methods are colorimetry [7], atomic absorption spectrometry [8, 9], electrothermal atomic absorption

spectrometry [10], cold vapor atomic absorption spectrometry [11], inductively coupled plasma emission spectrometry [12, 13], spectroscopy [14–16] and anodic stripping voltammetry [17], among them, fluorescence spectroscopy has the advantages of high sensitivity and simple operation, so it has attracted widespread attention, and many have been designed and synthesized probe [18].

Pyrazoline is an important nitrogen-containing five-membered heterocyclic compound. There are many methods to synthesize this compound [19–21] with many biological activities [22–28]. Pyrazoline has strong fluorescence properties, so it is also widely used in the field of optoelectronics. It is used as an optical brightener for textiles and papermaking materials. The pyrazoline fluorescent compound also has excellent stability, so it can be used in laser dyes, fluorescent dyes, for biological analysis, tracking detection, drug tracking and sun traps. Pyrazole is a colorless or white crystalline substance with high fluorescence quantum yield, high light stability, non-toxic and other optical properties, it is usually used as stabilizer, chelate, organic synthesis intermediate, etc [29–31]

Due to the excellent properties of pyrazole and pyrazoline, we designed and synthesized compound **M** that combines the advantages of both. This compound contains two fluorophores, a pyrazole unit and a pyrazoline unit. It has good selectivity and high-sensitivity fluorescence response to Fe<sup>3+</sup>.

**Electronic supplementary material** The online version of this article (<https://doi.org/10.1007/s10895-020-02632-w>) contains supplementary material, which is available to authorized users.

✉ Ying-Peng Zhang  
yingpengzhang@126.com

✉ Yun-Shang Yang  
yangyunshang@tom.com

<sup>1</sup> School of Petrochemical Engineering, Lanzhou University of Technology, Lanzhou 730050, China

<sup>2</sup> College of Chemistry and Chemical Engineering, Lanzhou University, Lanzhou 730000, China

In order to clarify the complex relationship between the probe and  $\text{Fe}^{3+}$ , theoretical calculations of density functional theory (DFT) were carried out. These results illustrate the reasonable design of fluorescent probes for  $\text{Fe}^{3+}$  detection. At the same time, the probe **M** has good yellow fluorescence, its emission wavelength is about 600 nm, the fluorescence quantum yield is high, the hole transport efficiency is high, it is easy to detect, and the color change can be directly observed with the naked eye. And it is also a good photoluminescent material. In addition, the resulting **M**- $\text{Fe}^{3+}$  group reacts specifically with pyrophosphate (PPI) anion through fluorescence quenching.

## Experimental Part

### Materials and Characterization

FA1004 Electronic Balance (Changzhou Nuoji Instrument Co., Ltd.); SGWX-4 Micro-melting Point Instrument (Shanghai Precision Scientific Instrument Co., Ltd.); Bruker-AV400, 400 MHz Nuclear Magnetic Resonance Instrument; HPLC Q-Tof HR-MS Mass Spectrometer (Waters Micromass); Bruker DTX-400 carbon spectrum analyzer; UV-1800PC spectrometer; HITACHIF-4500 fluorescence spectrometer.

During the experiment, various metal ions correspond to chloride salts ( $\text{Na}^+$ ,  $\text{K}^+$ ,  $\text{Ca}^{2+}$ ,  $\text{Cu}^{2+}$ ,  $\text{Zn}^{2+}$ ,  $\text{Ni}^{2+}$ ,  $\text{Pb}^{2+}$ ,  $\text{Mg}^{2+}$ ,  $\text{Al}^{3+}$ ,  $\text{Ba}^{2+}$ ,  $\text{Fe}^{3+}$ ,  $\text{Co}^{2+}$ ,  $\text{Mn}^{2+}$ ) and nitrate ( $\text{Ag}^+$ ). Other reagents are commercially available analytical grade, and all samples are performed at room temperature.

### Synthesis Route of Probe **M**

Scheme 1 shows the synthetic route of compound **M**.

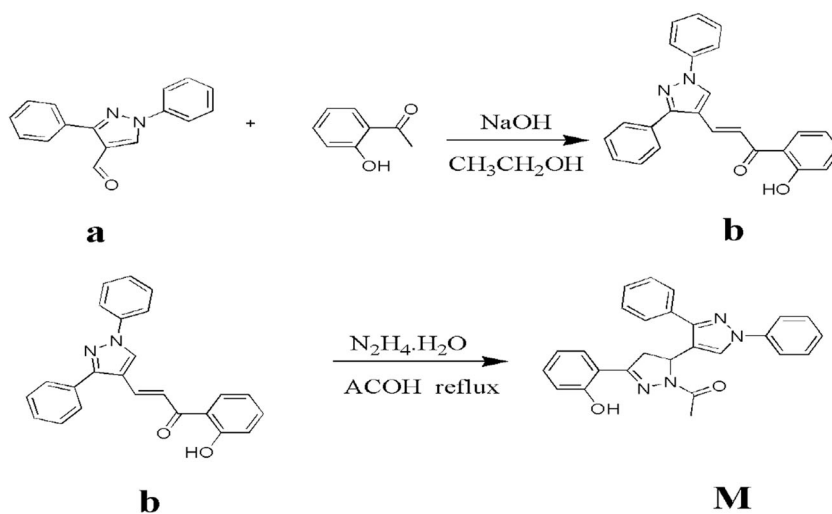
The synthesis of probe **M** is as follows: *o*-hydroxyacetophenone was purchased from a commercial

supplier. Compound **a** was prepared according to literature method [32] m.p.140–143 °C(lit [32]. m.p.144–146 °C), in 50 ml round-bottom flasks, add 0.210 g (1 mmol) of compound **a**, 0.136 g (1.0 mmol) of *o*-hydroxyacetophenone, 10 ml of ethanol and 1 ml of 10% NaOH at 75 °C was heated to reflux for 3 h. After the reaction was completed, it was cooled to room temperature to produce a bright yellow powder. The crude product was obtained by suction filtration. Recrystallized with V ethanol: V ethyl acetate (1:1) to obtain compound **b**. The rate is 88%. Dissolve 0.366 g (1.0 mmol) of compound **b** in 2 ml of acetic acid, completely dissolve it and transfer to an oil bath (120 °C), then add 1.0 ml of 80% hydrazine hydrate dropwise, heat for 4 h, and detect the completion of the reaction by TLC. After cooling to room temperature, white crystal **M** was produced with a yield of 78%, with a yield of 78%, mp: 230–233 °C The analysis data are as follows:  $^1\text{H NMR}$  ( $\text{CDCl}_3$ , 400 MHz)  $\delta$ ppm 2.39(s, 3H), 3.21(dd,  $J = 4.1, 4.0$  Hz, 1H), 3.71(d,  $J = 4.0$  Hz, 2H), 5.84(m, 1H), 6.87(t,  $J = 4.0$  Hz, 1H), 7.01(s, 2H), 7.25(s, 1H), 7.33(d,  $J = 3.1$  Hz, 2H), 7.41(dd,  $J = 5.1, 1.2$  Hz, 3H), 7.69(dd,  $J = 4.0, 2.3$  Hz, 4H), 7.81(s, 1H), 10.18(s, 1H).  $^{13}\text{C NMR}$  ( $\text{DMSO}-d_6$ , 100 MHz): 167.93, 156.59, 156.79, 154.00, 150.46, 146.86, 139.70, 136.81, 132.93, 131.40, 128.59, 126.99, 125.84, 119.69, 119.14, 117.45, 116.99, 115.73, 114.99, 112.44, 65.43, 50.86, 47.31, 42.41, 22.64, 22.13. calculated for  $[\text{M} + \text{H}]^+$  423.2411, found 423.2497.

### Spectral Test

The **M** mixed stock solution was prepared  $1.0 \times 10^{-3}$  M. The configuration of the cation stock solution is prepared from the corresponding chloride or nitrate. Make volume with soft water, the concentration is  $5.0 \times 10^{-3}$  M. Add 10  $\mu\text{L}$ , 20  $\mu\text{L}$  of Compound **M** solution ( $1 \times 10^{-3}$  M) to the cell, with an optical

**Scheme 1** Synthesis route of probe **M**



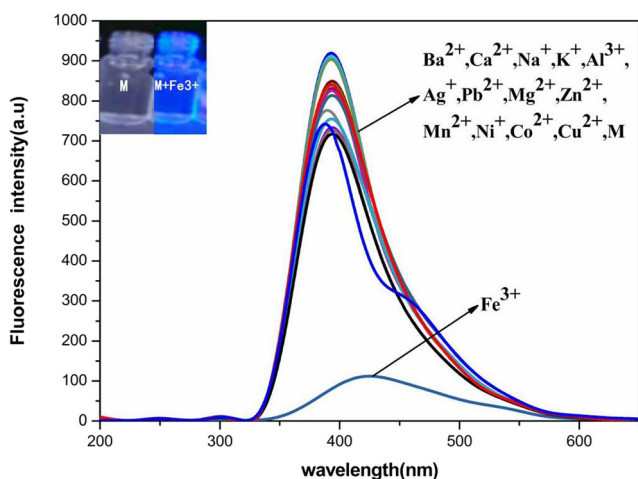


**Fig. 1** Fluorescence emission spectrum of **M** in THF / water mixed solvent (1: 1, v / v) containing HEPES buffer (0.02 mM, pH = 7.4) at room temperature

path of 1 cm, which contains 2 mL of THF/water (1:1 (v/v) and HEPES buffer (0.02 mM pH = 7.4), then add a certain amount of cation, and measure its UV-visible absorption, fluorescence spectrum and infrared spectrum.

## Results and Discussion

### Identification of Metal Ions by Probes

In the THF/water system, under the excitation wavelength of 280 nm, the probe showed strong fluorescence emission at 410 nm. The experimental results show that metal ions other than iron ions have little effect on the fluorescence of the system or have a very small fluorescence quenching effect (Fig. 1). This shows that probe **M** has a better response to iron ions.

**Table 1** Detection limits of Fe<sup>3+</sup> by other fluorescent sensors and fluorescent probe **M**

Fluorescence probes	Ions	Detection limits
1 [33]	Fe <sup>3+</sup>	1.05 × 10 <sup>-7</sup> M.
2 [34]	Fe <sup>3+</sup>	4.2 × 10 <sup>-8</sup> M.
3 [35]	Fe <sup>3+</sup>	2.54 × 10 <sup>-6</sup> M.
4 [36]	Fe <sup>3+</sup>	4.8 × 10 <sup>-6</sup> M.
5 [37]	Fe <sup>3+</sup>	6.5 × 10 <sup>-7</sup> M.
6 [38]	Fe <sup>3+</sup>	2.0 × 10 <sup>-3</sup> M.
Our probe <b>M</b>	Fe <sup>3+</sup>	3.9 × 10 <sup>-10</sup> M.

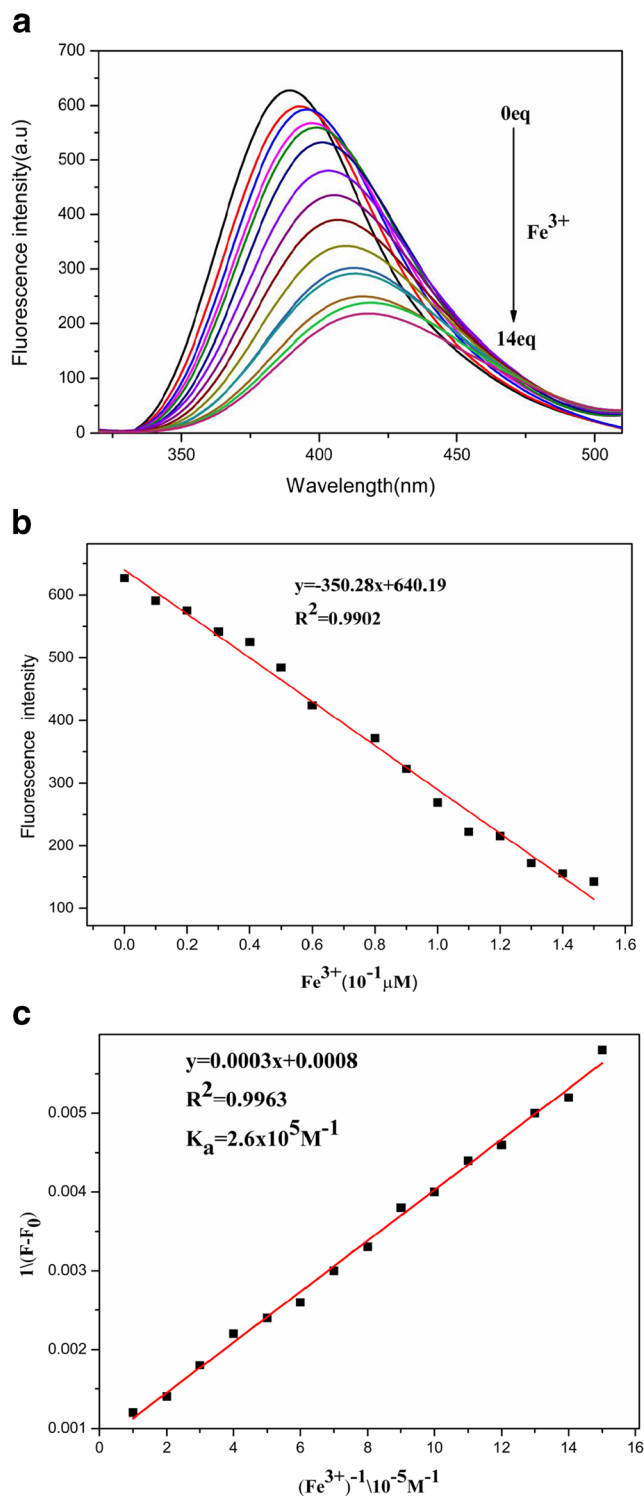


**Fig. 2** **a** Fluorescence emission intensity curve of adding different concentrations of Fe<sup>3+</sup> to probe **M**. **b** The fluorescence spectrum of the emission spectrum of probe **M** and the change in Fe<sup>3+</sup> concentration. **c** Complexation constant curve of Fe<sup>3+</sup> to probe **M** titration

### Fluorometric Titration Test of Iron Ion by Probe

Add a different multiple of iron ions to the probe in a THF/water (1:1: v/v) solution containing HEPES buffer (0.02 mM,

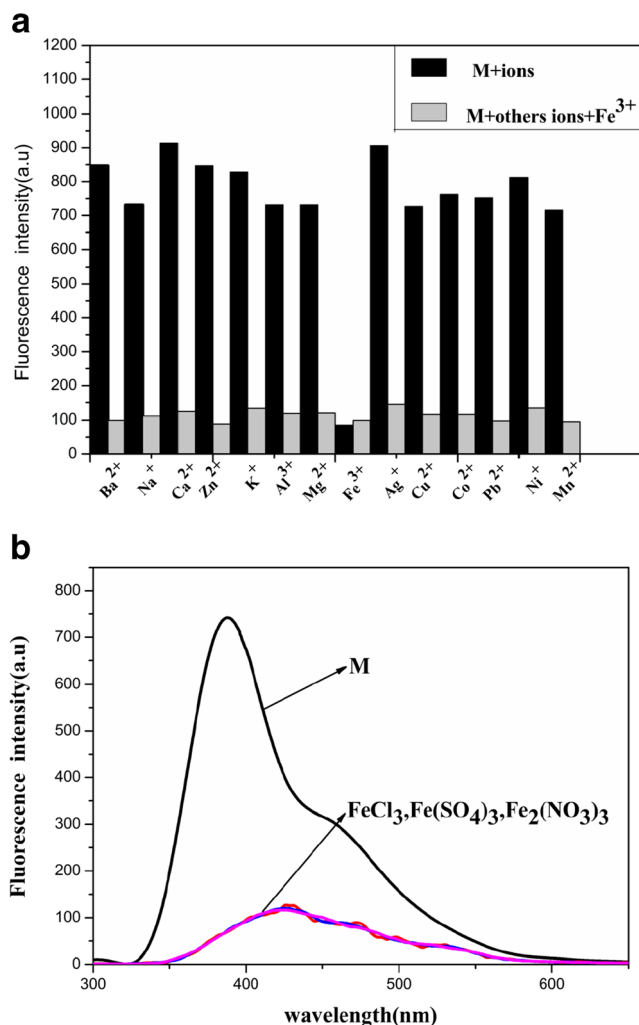


**Fig. 3** **a** In the presence of Fe<sup>3+</sup> and various other metal ions in a mixed solvent of THF/ water (1:1, v/v) containing HEPES buffer (0.02 mM, pH = 7.4) at room temperature Next, the fluorescence response of probe **M**. The black bar indicates the probe **M** plus other metal ion solutions. The gray bar indicates that the same amount of Fe<sup>3+</sup> is subsequently added to the mixture solution. **b** represents the fluorescence spectrum of probe **M** in a mixed solvent THF/water (1:1, v/v) containing HEPES buffer (0.02 mM, pH = 7.4) and different iron salts at room temperature

pH = 7.4), as shown in Fig. 2a, as the iron ion concentration as the factor increases, the fluorescence intensity of probe **M** decreases continuously until it reaches saturation. The quantitative response of probe **M** to Fe<sup>3+</sup> has a good linear relationship. As shown in Fig. 2b, the linear regression equation is  $y = 640.19 - 350.28x$ ,  $R^2 = 0.9902$ . The Benesi-Hildebrand non-linear curve fits a straight line, showing a linear fit, and confirms that the stoichiometric relationship between Fe<sup>3+</sup> and probe **M** is 1:1. From Fig. 2c, we can conclude that the binding constant of the **M**-Fe<sup>3+</sup> complex is  $2.6 \times 10^5 \text{ M}^{-1}$ . The

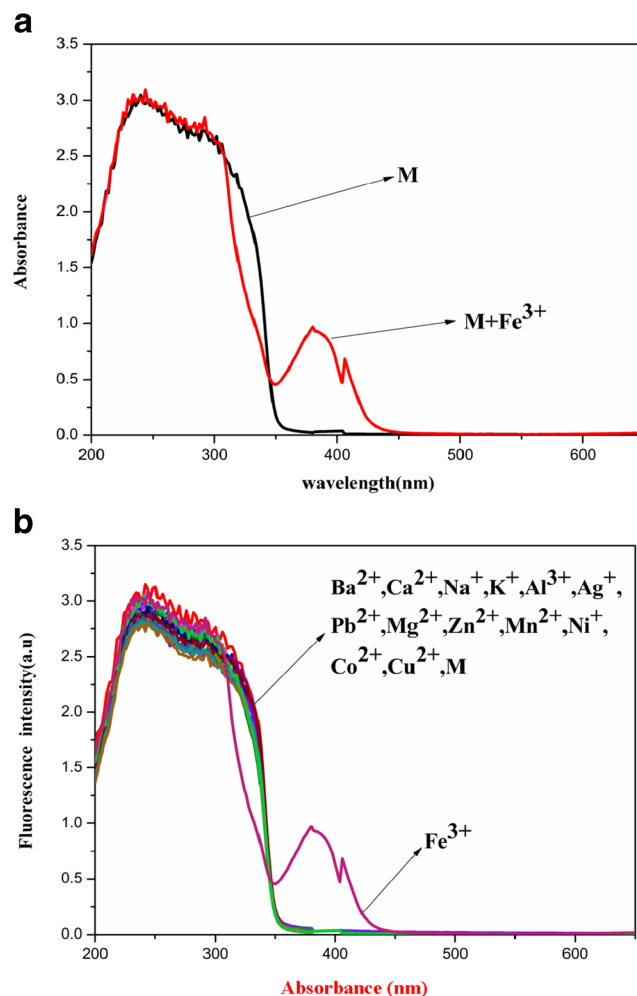


**Fig. 4** **a** UV-Vis spectra of probes **M** and **M** + Fe<sup>3+</sup> in THF/water (1:1, v/v) containing HEPES buffer (0.02 mM, pH = 7.4). **b** After adding various metal ions, the UV-visible spectrum of probe **M** changes

detection limit calculated from the multiple of the fluorescence intensity of the probe **M** relative to the standard deviation is  $3.9 \times 10^{-10} \text{ M}$  (when the probe concentration is  $1.0 \times 10^{-5} \text{ M}$ ). Table 1 lists several probes for Fe<sup>3+</sup> detection. Compared with the LOD of other probes, **M** probe has a lower detection line and a higher Fe<sup>3+</sup> detection sensitivity.

### Competitive Testing

In order to further detect the actual application of the probe **M** for the recognition of Fe<sup>3+</sup>, an anti-interference experiment was performed on the probe **M** (Fig. 3a). Only adding iron ions to the probe will significantly reduce the fluorescence intensity, and then add other

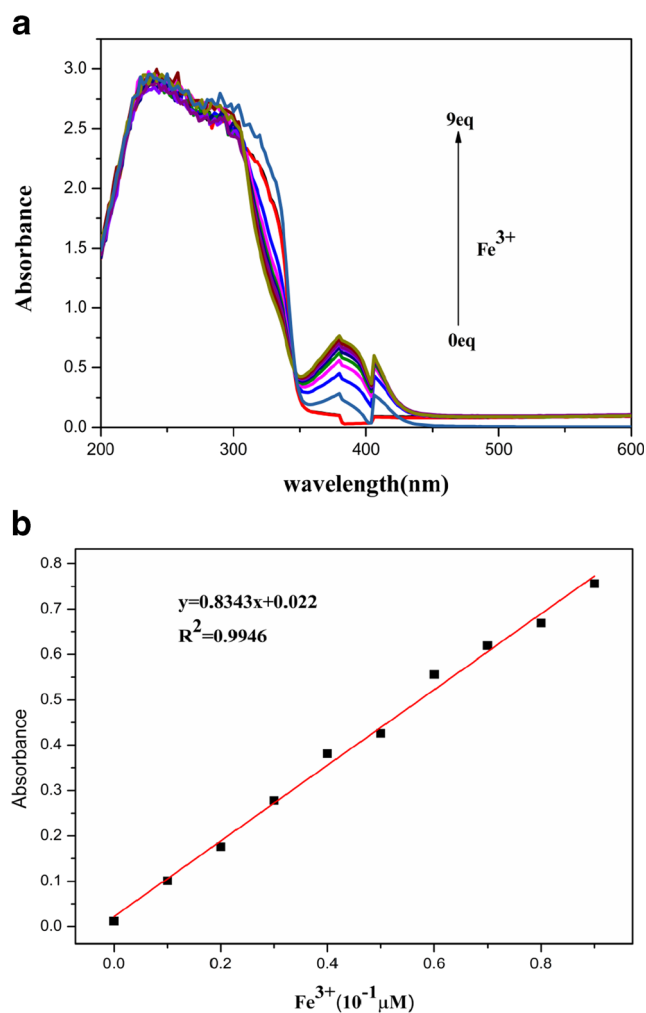


**Fig. 5a** UV absorption spectrum of fluorescent probe **M** and addition of different equivalents of  $\text{Fe}^{3+}$  metal ions. **b** Linear ultraviolet absorption spectrum of fluorescent probe **M** and iron ion concentration

equal amounts of metal ions. The fluorescence intensity remains basically unchanged. The results prove that the probe **M** does not interfere with other ions during the recognition process of  $\text{Fe}^{3+}$ , and has good anti-interference ability. In addition, in order to further explore the influence of anions on the identification process of iron ions in probe **M**, we configured iron sulfate ion, sulfate ion and chloride ion solutions in HEPES buffer (0.02 mM, pH = 7.4) THF /water Fluorescence spectroscopy tests were carried out in water (1:1: v/v) solution, as shown in Fig. 3b, the fluorescence response of the probe did not change significantly. The results show that in the process of identifying metal salt ions, anions will not affect the identification of metal ions.

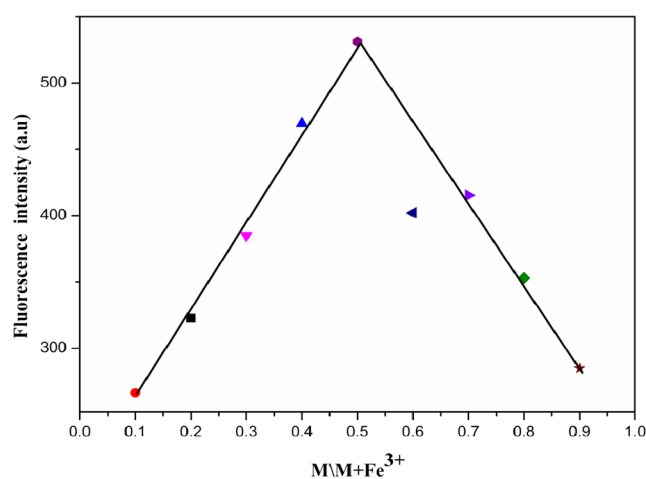


**Fig. 6** Used to determine the stoichiometry of probes **M** and  $\text{Fe}^{3+}$  in THF/water (1:1, v/v) with HEPES buffer (0.02 mM, pH = 7.4), total concentration  $1.0 \times 10^{-5}$  M Working graph

### Selective Features

In order to explore the practical application of probe **M** in a biological environment at room temperature, the absorption spectrum characteristics of probe **L** in a mixed solvent containing THF/water (1:1, v/v) for various metal ions were studied. As shown in Fig. 4a, without adding  $\text{Fe}^{3+}$  ions, the probe **M** showed a maximum absorption peak at 250 nm. Then,  $\text{Fe}^{3+}$  ions were added to the probe **M**. We found that it did cause a significant change in absorption, the absorbance at 310 nm increased, and a new band appeared at 310 nm. It can be clearly seen from Fig. 4b that when adding 1 eq  $\text{Fe}^{3+}$  and other metal ions ( $\text{Ba}^{2+}$ ,  $\text{Ca}^{2+}$ ,  $\text{Mg}^{2+}$ ,  $\text{Na}^+$ ,  $\text{Al}^{3+}$ ,  $\text{Mn}^{2+}$ ,  $\text{Ni}^+$ ,  $\text{Pb}^{2+}$ ,  $\text{Cu}^{2+}$ ,  $\text{Co}^{2+}$ ,  $\text{K}^+$ ,  $\text{Zn}^{2+}$ ,  $\text{Ag}^+$ , **M**), only  $\text{Fe}^{3+}$  The absorption peak has obvious changes.

### UV Absorption Spectrum of $\text{Fe}^{3+}$ Recognized by Probe

In THF/water (1:1, v/v) buffer containing HEPES (0.02 mM, pH = 7.4), as shown in Fig. 5a, adding different concentrations of  $\text{Fe}^{3+}$  ions, the probe **M** starts to absorb at 350 nm. It shows that a new complex is formed between compound **M** and  $\text{Fe}^{3+}$ . The UV-vis titration in Fig. 5b shows a good linear relationship between probe **M** and  $\text{Fe}^{3+}$ . The linear regression equation is  $y = 0.022 + 0.8343x$ ,  $R^2 = 0.9946$ . The spectral fit of the absorption data obtained with  $\text{Fe}^{3+}$  titration probe **M** shows that the stoichiometric ratio between probe **M** and  $\text{Fe}^{3+}$  is 1:1.

## Combination Ratio

In order to further explore the binding ratio of probe **M** to  $\text{Fe}^{3+}$ , the molar ratio of probe **M** to  $\text{Fe}^{3+}$  (9:1, 8:2, 7:3, 6:4, 5:5, 4:6, 3:7, 2:8, 1:9), to detect its fluorescence properties, and draw the curve shown in Fig. 6, the maximum molar fraction of probe **M** appears at 0.5, which supports the above 1:1 ( $\text{M}:\text{M} + \text{Fe}^{3+}$ ) in combination with stoichiometry.

## Detection Limit

The detection limit is calculated by  $\text{LOD} = 3\sigma/k$ , where  $\sigma$  is the standard deviation of the relative fluorescence intensity of the 15 sets of probes at the position of their emission peaks. After probe **M** is combined with different concentrations of  $\text{Fe}^{3+}$ , the emission peaks are relative to each other. The intensity is plotted against the corresponding concentration to ob-

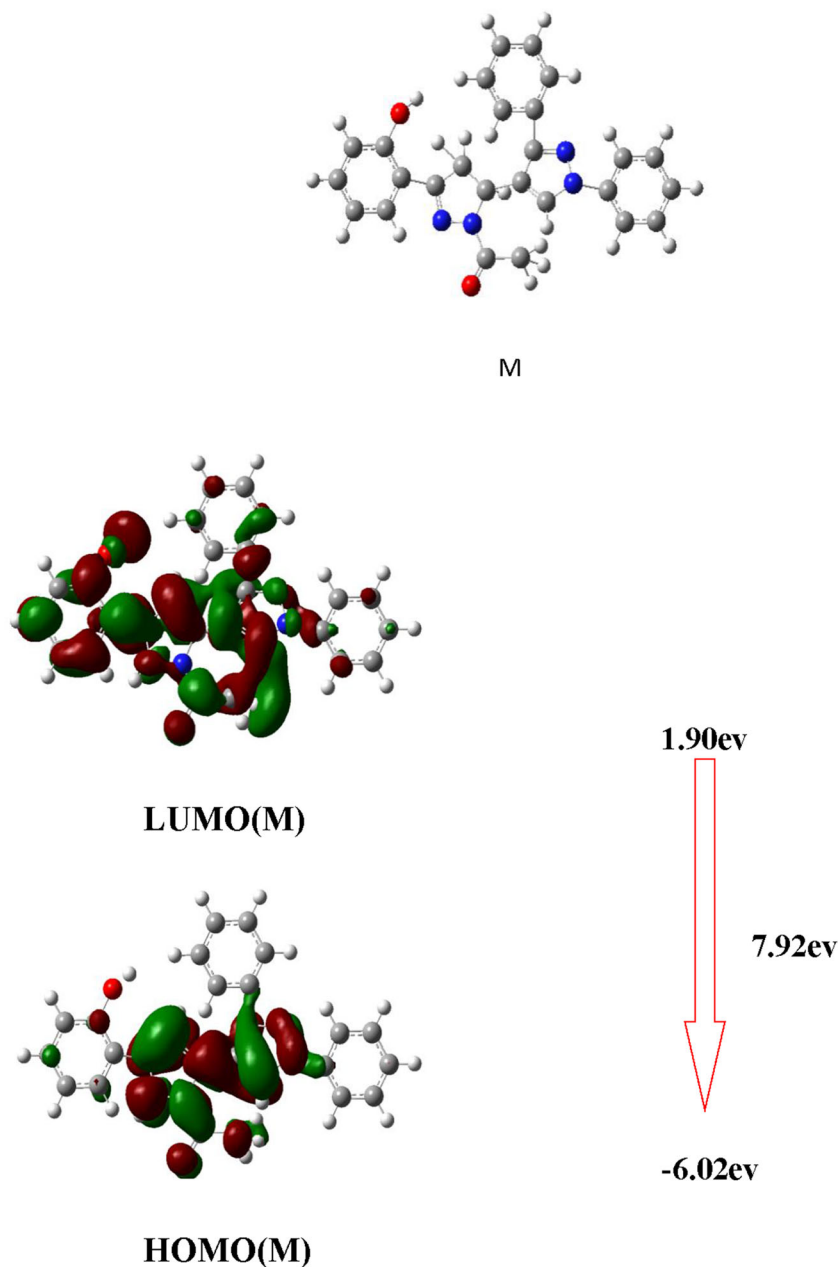


Fig. 7 Geometric optimization of Gaussian

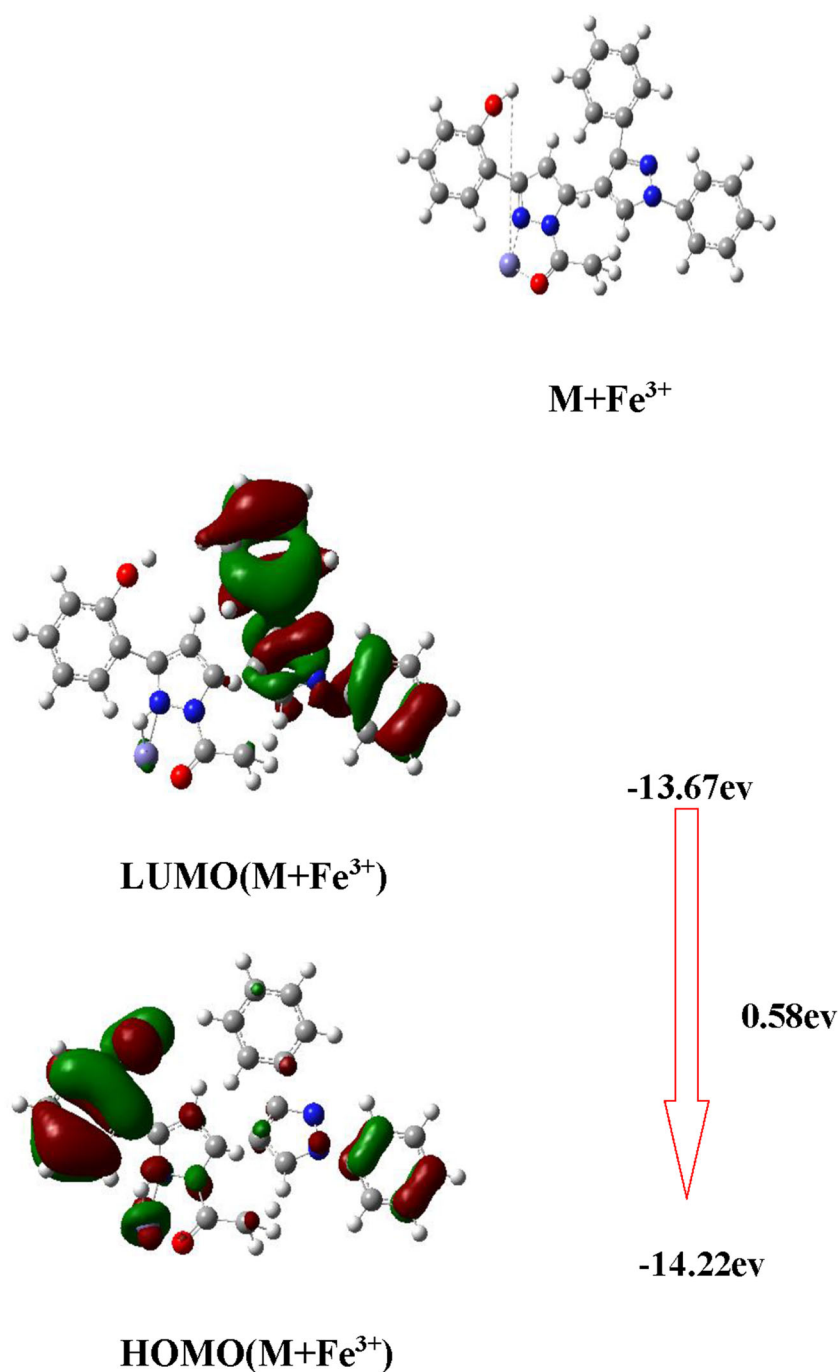


Fig. 8 (continued)

tain the slope  $k$ . Through calculation, the LOD of the probe **M** to  $\text{Fe}^{3+}$  is  $3.9 \times 10^{-10}\text{M}$ . Compared with the fluorescent probe for detecting  $\text{Fe}^{3+}$  listed in Table 1, the fluorescent probe **M** made by us has a lower detection limit.

### Optimized Calculation

To have a better understanding about the electronic structures of **M** and **M+Fe<sup>3+</sup>**, DFT calculations were

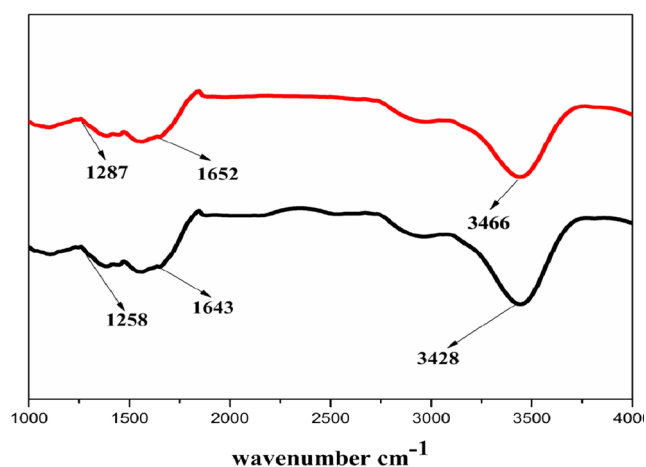


Fig. 8 Infrared spectra of probes **M** and **M + Fe<sup>3+</sup>**

performed at B3LYP/def2-SVP [39–41]. For the composite **M + Fe<sup>3+</sup>**, HOMO and LUMO are different from **M**. Due to the addition of **Fe<sup>3+</sup>** in pyrazoline, the HOMO of **M + Fe<sup>3+</sup>** is limited to this fragment, and the CT from the electron donor to the electron acceptor group is interrupted in **M + Fe<sup>3+</sup>**, resulting in a decrease in fluorescence. Compared with **M**, the LUMO-HOMO orbital energy of **M + Fe<sup>3+</sup>** is reduced (Fig. 7), and the acceptor system of the compound is destroyed. This is due to the hydrogen bonding interaction between C=N and C=O.

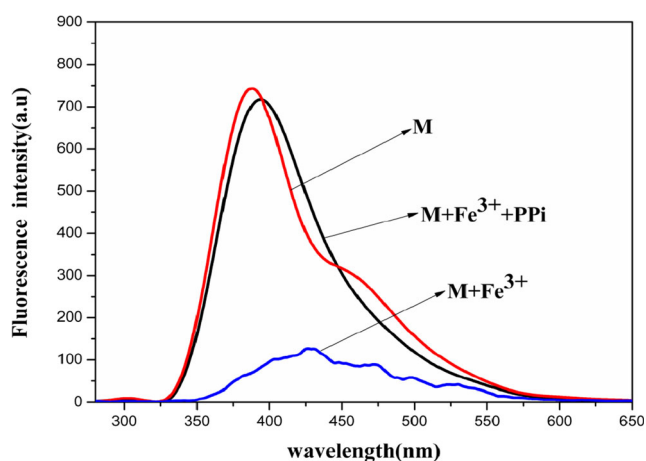


Fig. 9 Fluorescence spectrum of **M** combined with **Fe<sup>3+</sup>** when PPI was added to THF/water (1:1, v/v) containing HEPES buffer (0.02 mM, pH = 7.4)

## Infrared Spectrum Test

Figure 8 shows the FT-IR spectra of probes **M** and **M + Fe<sup>3+</sup>**. The characteristic bands of -OH, pyrazoline C=O and C=N extend at 3430  $\text{cm}^{-1}$ , 1664  $\text{cm}^{-1}$  and 1101  $\text{cm}^{-1}$ , respectively. After adding probe **M**, these three bands dropped from 3466  $\text{cm}^{-1}$ , 1652  $\text{cm}^{-1}$  and 1287  $\text{cm}^{-1}$  to 3428  $\text{cm}^{-1}$ , 1643  $\text{cm}^{-1}$  and 1258  $\text{cm}^{-1}$ , which may be due to -OH, C=O and C=N. The density of the group and **Fe<sup>3+</sup>** coordination electron cloud decreases [41].

## PPI Test Fluorescence Probe **M** Detection **Fe<sup>3+</sup>** Reversibility Experiment

By adding the chelating agent PPI to the fluorescent probe **M** to recognize the fluorescence emission peak of **Fe<sup>3+</sup>**, we can gain a deeper understanding of the response of the fluorescent probe **M** to **Fe<sup>3+</sup>**, as shown in Fig. 9, when adding PPI to the mixed solution of **M** and **Fe<sup>3+</sup>**. At this time, the fluorescence intensity of the complex almost quenches to the intensity of the fluorescent probe **M** itself, which shows that the complexation between the fluorescent probe **M** and **Fe<sup>3+</sup>** is reversible.

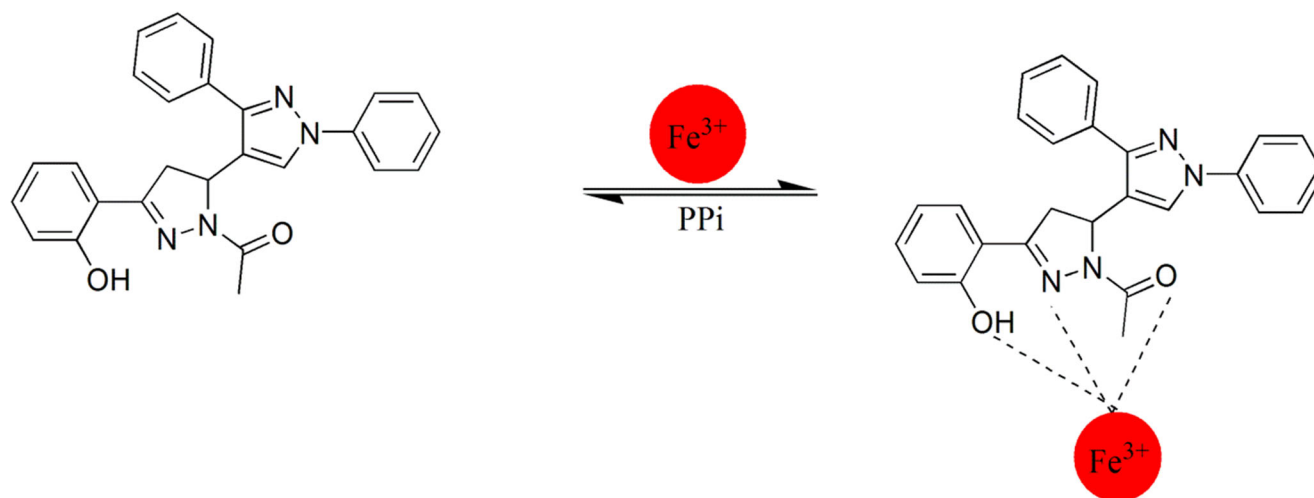
## Recognition Mechanism of Fluorescent Probe **M** and **Fe<sup>3+</sup>**

The possible binding mechanism of **M** with **Fe<sup>3+</sup>** induced the fluorescence changes is shown in Scheme 2. Based on the previously reported pyrazoline-based probes [42–44], we can speculate that **Fe<sup>3+</sup>** may interact with C=N, C=O and -OH on the fluorescent probe **M** to undergo photoinduced electron transfer and chelation. The cooperation thus weakens the binding of fluorescence [45], but the chelation of probe **M** with **Fe<sup>3+</sup>** makes the complex more rigid and limits the C=N isomerization [46, 47]. And because the binding ratio of probe **M** and **Fe<sup>3+</sup>** ions is 1:1, the phenomenon of fluorescence quenching is further confirmed and their binding mechanism.

## Conclusion

In summary, a novel fluorescent probe based on pyrazole-pyrazoline for Fe (III) ions recognition was designed and synthesized. By observing the ultraviolet absorption spectrum and fluorescence spectrum, it was found that tetrahydrofuran: water = 1:1 (v: v) in the presence of other metal ions, the probe **M** in the mixed solution has high selectivity, sensitivity and anti-interference ability for the detection of **Fe<sup>3+</sup>**, and the recognition process is reversible. The combination of probe **M**





**Scheme 2** The complexation mechanism between probe and ion is speculated

and iron ions is 1:1, and the detection limit is  $3.9 \times 10^{-10}$  M. The binding mode and sensing mechanism of **M** with  $\text{Fe}^{3+}$  was verified by theoretical calculations using Gaussian 09 based on B3LYP/6-31G(d) basis.

## References

- DeSilva AP, Gunaratne HQN, Gunlaugsson T et al (1997) The stability of cyclodextrin complexes in solution. *Chem Rev* 97: 1514–1566
- Aisen P, Wessling-Resnick M, Leibold EA (1999) Iron metabolism. *Curr Opin. Chem Biol* 3:200–206
- Touati D (2000) Iron and oxidative stress in bacteria. *Arch Biochem Biophys* 373:1–6
- Bharath S, Hsu M, Kaur D, Rajagopalan S, Andersen JK (2002) Glutathione iron and Parkinsons disease. *Biochem Pharmacol* 64(5):1037–1048
- Honda K, Casadesus G, Petersen RB et al (2004) Oxidative stress and redox-active iron in alzheimers disease. *Ann N Y Acad Sci* 1012(1):179–182
- Narayanaswanmy N, Govindaraju T (2012) Aldazine-based colorimetric sensors for  $\text{Cu}^{2+}$  and  $\text{Fe}^{3+}$ . *Chemical* 161(1):304–310
- Liang ZO, Wang CX, Yang JX, et.al. A highly selective colorimetric chemosensor for detecting the respective amounts of iron(II) and iron (II) irons in water. *New J Chem* 2007;31(6):906–910
- González APS, Firmino MA, Nomura CS, Rocha FRP, Oliveira PV, Gaubeur I (2009) Peat as a natural solid-phase for copper preconcentration and determination in a multicommuted flow system coupled to flame atomic absorption spectrometry. *Anal Chim Acta* 636(2):198–194
- Mashhadizadeh MH, Pesteh M, Talakesh M, Sheikhshoae I, Ardakani MM, Karimi MA Solid phase extraction of copper (II) by sorption on octadecyl silica membrane disk modified with a new Schiff base and determination with atomic absorption spectrometry. *Spectrochimica Acta Part B Atomic Spectroscopy* 2008;63(8):885–8, 888
- Liu J, Yu M, Wang XC, Zhang Z (2012) A highly selective colorimetric sensor for  $\text{Hg}^{2+}$  based on nitrophenyl-aminothiourea. *Spectrochim Acta A* 93(10):245–249
- Gupta VK, Singh AK, Mergu N (2014) Antipyrine based schiff bases as turn-on fluorescent sensors for Al (III) ion. *Electrochim Acta* 117(4):405–412
- Liu Y, Liang P, Guo L (2005) Nanometer titanium dioxide immobilized on silica gel as sorbent for preconcentration of metal ions prior to their determination by inductively coupled plasma atomic emission spectrometry. *Talanta* 68(1):25–30
- Ferreira SLC, Queiroz AS, Fernandes MS, dos Santos HC (2002) Application of factorial designs and doehlert matrix in optimization of experimental variables associated with the preconcentration and determination of vanadium and copper in seawater by inductively coupled plasma optical emission spectrometry. *Spectrochimica Acta Part B Atomic Spectroscopy* 57(12):1939–1950
- Tesfaldef ZO, Vanstaden JF, Stefan RI (2004) Sequential injecting spectrophotometric determination of irons as Fe(II) in multi-vitamin preparations using 1, 10-phenanthroline as complexing agent. *Talanta* 64(5):1189–1195
- Gomes D, Segundo M, Lima J et al (2005) Spectrophotometric determination of iron and boron in soil extracts using a multi-syringe flow injecting system. *Talanta* 66(3):703–711
- Lunvongsa S, Oshima M, Motomizu S (2006) Determination of total and dissolved amount of iron in water samples using catalytic spectrophotometric flow injecting analysis. *Talanta* 68(3):969–973
- Mohadesi A, Taher MA. Voltammetric determination of cu(II) in naturalwaters and human hair at a meso-2,3-dimercaptosuccinic acid self-assembled gold electrode. *Talanta* 2007;72(1):95–0, 100
- Sahoo SK, Sharma D, Bera RK et al (2012) Iron (III) selective molecular and supramolecular fluorescent probes. *Chem Soc Rev* 41(21):7195–7227
- Levai A, Jeko J (2006) Synthesis of 1-Substituted 5-Aryl-3-styryl-2-pyrazolines and 3-Aryl-5-styryl-2-pyrazolines by the Reaction of Dibenzylideneacetones and E.E-Cinnamylideneacetophenones with Hydrazines. *J Heterocyclic Chem* 43:1303–1309
- Wiley KH (1967) Pyrazles, Pyrazolines, Pyrazolidnes, Indazoles and Condensed rings. *The Chemistry of Heterocyclic Compounds* 20:180–188
- Levai A (2002) Synthesis of 3-Aroyl-4-(3-chromony)-2-pyrazolines. *J Heterocyclic Chem* 39:1333–1336
- Khali HZ, Yanni SA (1981) Synthesis of new Anilido-Pyrazoline and Isoxazoline Derivatines. *J Indian Chem Soc* 58:168–170
- Rawal AA, Thakor VM, Shah NM (1963) Synthesis of some 1, 3,5-Triphenylpyrazolines and 3,5-Diphenyl-cyclohexen-1-ones. *J Indian Chem Soc* 40(4):323

24. Dhal PN, Acharya TE, Nayak A (1975) Studies on 1,3-Diaryl Pyrazolines and their derivatives. *J Indian Chem Soc* 52:1196–1198
25. Bhatia MS, Sood RK (1978) New heterocyclic ring containing phosphorus: synthesis of 4-Chloro-1,4-dihydro-2 H-naphth-[2,1-c][1,2] oxaphosphorin. *Ind J Chem* 16B:638–645
26. Turan-Zitouni G, Chevallet P, Kilic FS, Erol K (2000) Synthesis of some thiazolyl-pyrazoline derivatives and preliminary investigation of their hypotensive activity. *Eur J Med Chem* 35:635–641
27. Erhan R, Mutlu A, Tayfun U, Dilek E (2001) Synthesis and antidepressant activities of some 3,5-diphenyl-2-pyrazolines. *Eur J Med Chem* 36:539–543
28. Husain MI, Shukla S (1986) Synthesis & biological activity of 4-(3-Aryl-4-exo-2-thioxothiazolidin-5-ylimino)-3-methyl-1-(N,N-disubstituted amino-methyl)pyrazolin-5-ones. *Ind J Chem* 25B:983–985
29. Orrego-Hernández J, Portilla J (2017) Synthesis of dicyanovinyl-substituted 1-(2-pyridyl) pyrazoles: design of a fluorescent chemosensor for selective recognition of cyanide. *J Org Chem* 82(24):13376–13385
30. Ibnaouf KH, Elzupir AO, Ibrahim MA, Ali MKM, Al-Muhanna MK (2019) Optical characteristics and structural properties of 3-(p-Nitrophenyl)-5-phenyl-1H-pyrazole. *J Electron Mater* 48(2):861–866
31. Maliyappa MR, Keshavayya J, Mahanthappa M, Shivaraj Y, Basavarajappa KV (2020) 6-substituted benzothiazole based dispersed azo dyes having pyrazole moiety: synthesis, characterization, electrochemical and DFT studies. *J Mol Struct* 1199:126959
32. Orrego-Hernandez J, Portilla J (2017) Synthesis of Dicyanovinyl-substituted 1-(2-Pyridyl)pyrazoles: Design of a Fluorescent Chemosensor for selective recognition of cyanide. *J Org Chem* 82:13376–13385
33. Wang CC, Zhang D, Huang XY, Ding P, Wang Z, Zhao Y, Ye Y (2014) A fluorescence ratiometric chemosensor for Fe<sup>3+</sup> based on TBET and its application in living cells. *Talanta* 128:69–74
34. Jin XD, Wang SF, Yin WZ, Xu T, Jiang Y, Liao Q, Xia X, Liu J (2017) A highly sensitive and selective fluorescence chemosensor for Fe<sup>3+</sup> based on rhodamine and its application in vivo imaging. *Sensors Actuators B* 247:461–468
35. Bozkurt E, Arik M, Onagner Y (2015) A novel system for Fe<sup>3+</sup> ion detection based on fluorescence resonance energy transfer. *Sensors Actuators B* 221:136–147
36. Zhao B, Liu T, Fang T et al (2017) A new selective chemosensors based on phenanthro[9,10-d] imidazole-coumarin with sequential “on-off-on” fluorescence response to Fe<sup>3+</sup> and phosphate anions and its application in living cells. *Sensors Actuators B* 246:370–379
37. Li P, Zhang M, Sun XK, Guan S, Zhang G, Baumgarten M, Müllen K (2016) A dendrimer-based highly sensitive and selective fluorescence-quenching sensor for Fe<sup>3+</sup> both in solution and as film. *Biosens Bioelectron* 85:785–791
38. Sen S, Sarkar S, Chattopadhyay B, Moirangthem A, Basu A, Dhara K, Chattopadhyay P (2012) A ratiometric fluorescence chemosensor for iron: discrimination of Fe<sup>2+</sup> and Fe<sup>3+</sup> and living cell application. *Analyst* 137:3335–3342
39. Becke AD (1988) Density-functional exchange-energy approximation with correct asymptotic behaviour. *J Phys Rev A* 38:3098–3000
40. Becke AD (1993) Density-functional thermochemistry III the role of exact exchange. *J Chem Phys* 98:5648–5652
41. Lee C, Yang W, Parr RG (1988) Development of the Colle-Salvetti correlation-energy formula into a function of the electron density. *Phys Rev B* 37:785–789
42. Zhang TT, Wang FW, Li MM, Liu JT, Miao JY, Zhao BX (2013) A simple pyrazoline-based fluorescent probe for Zn<sup>2+</sup> in aqueous solution and imaging in living neuron cells. *Sensors Actuators B* 186:755–760
43. Kasirajan G, Krishnaswamy V, Raju N, Mahalingam M, Sadasivam M, Palathurai Subramaniam M, Ramasamy S (2017) New pyrazolo-quinoline scaffold as a reversible colorimetric fluorescent probe for selective detection of Zn<sup>2+</sup> ions and its imaging in live cells. *Journal of Photochemistry and Photobiology A* 341:136–145
44. Li MM, Wang FW, Wang XY, Zhang TT, Xu Y, Xiao Y, Miao JY, Zhao BX (2014) A new turn-on fluorescence probe for Zn<sup>2+</sup> in aqueous solution and imaging application in living cells. *Anal Chim Acta* 826:77–83
45. Mikata Y, Yamashita A, Kawamura A et al (2009) Bisquinoline-based fluorescent zinc sensors. *Dalton Trans* 19:3800–3806
46. Maity D, Govindaraju T (2011) Naphthaldehyde-urea/thiourea conjugates as turn-on fluorescent probes for Al<sup>3+</sup> based on restricted C=N isomerization. *Eur J Inorg Chem* 36:5479–5485
47. Velmurugan K, Raman A, Easwaramoorthi S, Nandhakumar R (2014) Pyrene pyridine-conjugate as Ag selective fluorescent chemosensor. *RSC Adv* 4:35284–35289

**Publisher's Note** Springer Nature remains neutral with regard to jurisdictional claims in published maps and institutional affiliations.